


Maren Zimmermann
Carola Raffel
Jens Bartsch
Markus Thommes*

Simulation of Powder Flow Behavior in an Artificial Feed Frame Using an Euler-Euler Model

The Eulerian approach is an alternative numerical method to the traditionally used discrete particle techniques for modeling powder flow, avoiding limitations on particle number and diameter. The feasibility of an Euler-Euler simulation in a pharmaceutical application was investigated. In two- and three-dimensional flow simulations, computational fluid dynamics models and parameters were determined and verified based on comparison with experiments. Residence time distributions were calculated to show the applicability of the Eulerian model with two granular phases under the constraint of a continuous setup. Finally, this model was implemented to improve the process understanding of the powder flow in an artificial feed frame of a rotary tablet press.

 This is an open access article under the terms of the Creative Commons Attribution License, which permits use, distribution and reproduction in any medium, provided the original work is properly cited.

Keywords: Euler-Euler simulations, Feed frames, Granular phases, Powder flows

Received: November 12, 2021; *accepted:* February 28, 2022

DOI: 10.1002/ceat.202100580

1 Introduction

Tablets are the most common dosage form for the administration of active pharmaceutical ingredients (APIs), as they offer numerous advantages including high patient compliance, ease of handling, and excellent dosing accuracy [1, 2]. To enable production capacities in excess of one million tablets per hour, tablets are mainly produced on rotary tablet presses [2]. Most rotary tablet presses contain a feed frame with rotating paddles to facilitate the powder flow into the dies [3]. As powder particles and, hence, the product can be influenced by the residence time in the feed frame, knowledge of the powder flow as well as the residence time distribution (RTD) is essential for tablet manufacturing [3–5]. Here, the ascending slope of the cumulative density function F^1 , which gives the total discharged amount of tracer as a function of time [6], characterizes the mixing behavior of the powder particles.

In the context of pharmaceutical production, the systematic approach of quality-by-design (QbD) was implemented according to the guidelines of the International Conference on Harmonization (ICH) [7]. The goal of the concept is ensuring and building quality into products throughout the manufacturing process based on the correlation of material, as well as process parameters, to the quality of the product [8]. In general, an in-depth product and process understanding is emphasized for the implementation of QbD [9]. Different tools to use the QbD approach are available, such as process analytical technology and numerical simulations [10].

For gaining insights into the powder flow in a feed frame via numerical simulation, the most commonly used method is the discrete element method (DEM) [11–18]. DEM is a Lagrangian method, which is based on individually tracking each particle [19]. The application of the Lagrangian method is advantageous for getting detailed particle-scaled information, such as particle trajectories [14, 20]. This numerical method requires a high degree of computational power, which is dependent on the number of particles [21]. For simulating powder flows in pharmaceutical applications, particle sizes were frequently increased or studies focused only on small domains to reduce the number of particles and, thereby, the computational effort [13, 15, 22]. However, altering the particle characteristics could potentially influence the result of a numerical simulation, resulting in a false representation of the actual mechanism.

The Eulerian approach is an alternative numerical method for simulating the powder flow that has been evaluated in literature [23–26]. Contrary to the Lagrangian method, the solid phase is treated mathematically as an interpenetrating continuum with representative properties. The kinetics and the rheology of the particles are modeled by supplementary closure equations [23, 26]. Simulations using the Eulerian model are not limited by the number of particles, which is the main advantage of this model. Additionally, the Eulerian approach

Maren Zimmermann, Carola Raffel, Dr. Jens Bartsch, Prof. Markus Thommes
professors.fsv.bci@tu-dortmund.de
TU Dortmund University, Laboratory of Solids Process Engineering,
Department of Biochemical and Chemical Engineering, Emil-Figge-
Strasse 68, 44227 Dortmund, Germany.

1) List of symbols at the end of the paper.

provides better convergence behavior compared to the Lagrangian model [23].

The aim of this study is to investigate the feasibility of modeling particulate flow by using the Eulerian approach with granular phases. The simulation models and parameters are determined by comparing two-dimensional flow simulations with experimental data. In a subsequent step, the simulation setup is transferred and verified on a geometry with increased complexity. Finally, RTDs in a feed frame are calculated using the Eulerian approach to increase both time- and cost-efficiency with respect to the Lagrangian model and experiments, respectively.

2 Materials and Methods

2.1 Materials

The materials used in this study included dicalcium phosphate anhydrate (DI-CAFOS, DI-CAFOS A150, Chemische Fabrik Budenheim, Budenheim, Germany), microcrystalline cellulose (MCC, EMCOCEL 90M, JRS, Rosenberg, Germany), and Eosin Y (Merck, Darmstadt, Germany). All materials were used as received. The tracer formulation, consisting of 0.1 % (m/m) Eosin Y, was blended in a tumbling mixer (T 10 B Turbula, WAB, Muttenz, Switzerland) in batches of 2 kg each (32 rpm, 10 min, 10-L mixing bin).

2.2 Computational Methodology

In this work, an Eulerian multiphase model with a granular phase was employed [25, 27, 28]. For specifying the particulate flow, the differential equations for mass and momentum conservation, as well as the constitution equations based on the kinetic theory of granular flows, are solved for each phase. Exchange coefficients, which are modeled empirically, are used to calculate the interphase force between the gaseous and the particulate phase [27]. The models for the granular phase, which were chosen based on theoretical assumptions, are listed in Tab. 1.

2.3 Simulation Setup

In the simulation, a gaseous and a granular phase were modeled using the Eulerian approach. The gaseous phase described the air, and the granular phase consisted of DI-CAFOS or MCC. The particles were considered monodisperse, ideal spheres. The simulation properties of the granular phase are listed in Tab. 2.

Table 1. Simulation models for the granular phase of the Eulerian-Eulerian simulation.

Phase properties	Simulation model
Drag model	Schiller and Naumann [29]
Solids pressure	Lun [30]
Collisional viscosity	Gidaspow [31]
Kinetic viscosity	Lun [30]
Frictional viscosity	Schäffer [32]
Bulk viscosity	Lun [30]
Frictional pressure	Kinetic theory [27]

The angle of internal friction γ of the granular phase and the coefficient of restitution e between the particles were fitted by comparing the simulation with the corresponding calibration experiments using the method of least squares. In general, γ had a minor influence on the simulation result. The values (Tab. 2) were in good agreement with the non-compacted and dynamic condition of the powder bulk. In contrast, the result of the simulation was affected strongly by the coefficient of restitution. An increase in e caused a higher degree of interaction between the particles, which is in accordance with experimentally determined literature data [33, 34].

Two geometries were used to analyze the applicability of the Euler-Euler approach, i.e., a two-dimensional funnel and a three-dimensional feed frame with a rotating stir-type agitator. The size of the geometries equated to the experimental dimensions (Fig. 1). Different meshes, which consisted of tetrahedrons, were created. Mesh independency was proven for all geometries.

The outlet of the geometry was defined as a pressure outlet to enable powder discharge. The inlet was defined as a mass-flow inlet. A no-slip condition was applied between the granular material and the wall. For the simulation of the funnel, the axial symmetry of the geometry enabled the simulation of only half of the geometry. In the second investigated geometry, a feed frame, the paddle type-agitator rotated with varying speed.

For the initialization of the computational domains, the particulate phase was stacked to form a loose bulk with the friction packing limit of the material. The mass flow rate of the granular phase at the inlet was set to zero for measuring the time of powder discharge. In contrast, it was adjusted accordingly to ensure an equal powder bed height during the continuous simulation for determining the RTD.

In the commercial software package FLUENT 19.3 (ANSYS, Inc., Canonsburg, USA), the model equations were solved using a pressure-based solver with a finite volume method [27].

Table 2. Simulation setup for the granular phase of the Eulerian-Eulerian simulation.

Material	Particle diameter d_p [μm]	Density ρ [kg m^{-3}]	Friction packing limit [-]	Packing limit [-]	Angle of internal friction γ [$^\circ$]	Coefficient of restitution e [-]
DI-CAFOS	170	2890	0.2536	0.2779	63	0.54
MCC	130	1500	0.2340	0.2830	75	0.94

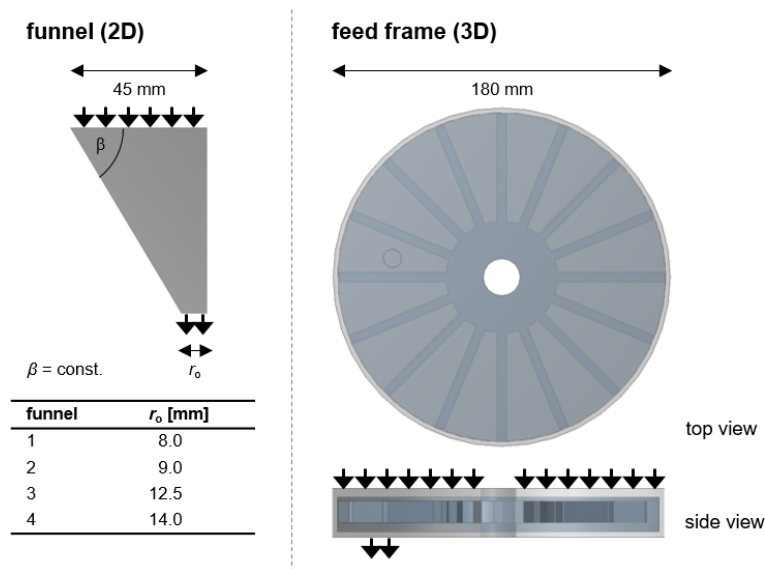


Figure 1. Two-dimensional funnel and three-dimensional feed frame for the simulation of powder discharge and determination of the RTD.

The pressure-velocity coupling was realized by the SIMPLE-algorithm. For spatial discretization, the first-order upwind scheme was used. The time-step size was set to 10^{-4} s and 10^{-3} s in the two- and three-dimensional simulations, respectively. Time-step size independence of the simulations was verified. The threshold of the residual values was 10^{-3} . For lower residual values, convergence was assumed.

2.4 Experimental Settings

For the selection of the simulation parameters and the verification of the simulation results, experiments with the same conditions compared to the simulations were conducted. In comparison to the two-dimensional simulation, the powder heights in the funnels of the experiment were equal to ensure the same powder mass ($m_{\text{DI-CAFOS,funnel}} = 100$ g, $m_{\text{MCC,funnel}} = 40$ g). Four different funnels were used. The time for the powder discharge was measured six times. Additionally, the powder outflow from the feed frame was determined for six rotational speeds of the stir-type agitator (10, 20, 30, 60, 90, and 120 rpm). The same initial mass load for the experiments and the simulation was used ($m_{\text{DI-CAFOS,feed frame}} = 250$ g, $m_{\text{MCC,feed frame}} = 150$ g) and the experiments were conducted six times.

For RTD determination, different powder layers of pure material and tracer formulation were stacked in the feed frame in the initial state. Experiments were conducted with three different rotational speeds (10, 30, 90 rpm). During the experiments, samples were taken every 10 s over a period of 2 min. For analysis, a powder sample ($m_{\text{powder}} = 500$ mg) was dissolved in 20 mL demineralized water. Solid residuals were removed by centrifugation (Centrifuge 5418, Eppendorf AG, Hamburg, Germany). The supernatant was diluted, and the amount of theophylline was quantified by UV absorption (Biomate 3, Thermo Fisher Scientific, Waltham, USA) at 272 nm. Each tracer concentration measurement was conducted in triplicate.

3 Results and Discussion

3.1 Determination of Material Parameters for the Eulerian Simulation

For verification of the chosen simulation models and parameters, both the simulated and measured time of powder discharge $t_{\text{discharge}}$ from four funnels for DI-CAFOS and MCC are plotted in Fig. 2. In all cases, the initial powder mass in the simulation and the experiment were equal.

According to Fig. 2, an increasing radius of the funnel outlet led to a shorter powder discharge time. In comparison, a slower powder outflow of MCC compared to DI-CAFOS, was observed. For funnels 1 and 2, $t_{\text{discharge}}$ of MCC could not be measured, as the outlet was clogged by the particles. Overall, the results of the simulation represent the experimentally determined results well, based on a maximum difference in $t_{\text{discharge}}$ of 7.95 % (DI-CAFOS, funnel 2). Consequently, the applicability

of the Eulerian model with a granular phase is reasonable for the description of the powder behavior. No constraints regarding particle number and diameter could be detected. However, a limitation for static powder conditions was observed: it was not possible to predict the clogging of the funnel opening for MCC. This might be due to the fact that the calculation of the frictional pressure was based on the kinetic theory. This model seems to be suitable for describing dynamic processes of a granular phase but might underestimate the frictional viscosity and, hence, the solid shear stress at the maximum packing limit.

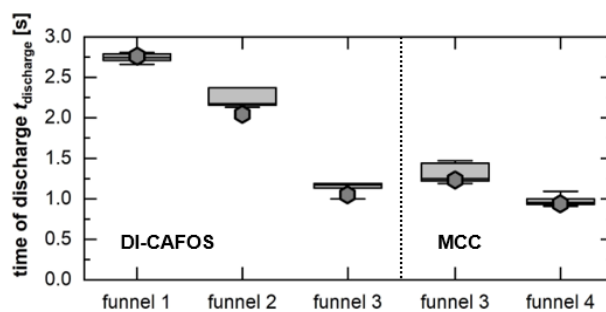


Figure 2. Experimentally determined (box plot, filled area between the 25th and the 75th percentile, whiskers from minimum to maximum, median, $n = 6$) and simulated (dark grey hexagon) time of powder discharge $t_{\text{discharge}}$ from funnels with different outlet radii ($r_{o,1} < r_{o,4}$) for DI-CAFOS and MCC.

3.2 Verification of Simulated Powder Flow

The simulation models and parameters were transferred from the two- to a three-dimensional geometry with a rotating stir-type agitator to prove the applicability of the Eulerian model. The results of the mean powder flow \dot{m} from the feed frame for

both the simulation and the experiment as a function of the rotational speeds of the agitator are presented in Fig. 3.

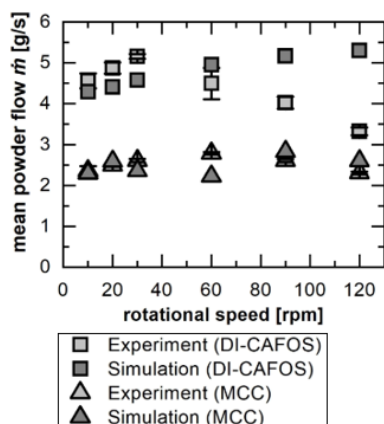


Figure 3. Experimentally determined ($mean \pm s$, $n = 6$) and simulated mean powder flow \dot{m} ($t = 30$ s) from a feed frame as function of rotational speed for DI-CAFOS and MCC.

In general, the mass flow for DI-CAFOS exceeded the mass flow for MCC due to a higher flowability. Additionally, an increase in the powder flow was caused by an increasing rotational speed. Rotational speeds of 90 and 120 rpm for the material DI-CAFOS were exceptions. For these experimental settings, the particles were affected by high centrifugal forces, which were generated by the fast agitator. Hence, the particles were forced towards the wall. Because of the existing dead volume between the wall and the agitator, the mass flow was reduced. The effect was only significant for DI-CAFOS as the flowability of MCC is lower.

Similar to the results of the two-dimensional simulation, the three-dimensional simulation describes the experimentally determined powder flow from the feed frame well (Fig. 3), which demonstrates the applicability of the Eulerian approach to describe a particulate phase. For DI-CAFOS as an example of a free-flowing material, deviations were observed for high paddle speeds, since the effect of the centrifugal forces cannot be presented adequately in the simulation. However, the apparent limitation is not relevant practically speaking due to the handling of maximum easy-flowing materials like MCC or the use of lower rotational speeds.

3.3 Simulation of Residence Time Distribution

For investigating the feasibility of the Eulerian model with two granular phases, the RTDs in the feed

frame were simulated and compared to experimentally determined profiles. The distributions were analyzed as a function of dimensionless time to avoid possible inaccuracies caused by deviations in mass flow between simulation and experiment. Measurements were conducted three times for one experimental setup (DI-CAFOS, 30 rpm). Due to a small standard deviation in the location parameter (2.24%) and the width of the distribution (2.62%) between the repeated measurements, repeatability was assumed for all experiments.

In a discontinuous simulation setup, two granular phases (pure material and tracer formulation) were layered in the geometry. Both granular phases consisted of the same material, and thus, had the same simulation parameters. The ascending curve of the simulated and experimentally determined F profiles were comparable, which highlights the feasibility of the overall approach to predict the mixing behavior of two granular phases in a steady state by the Eulerian approach. However, the maximum tracer concentration was reached after a short period. This overestimation of the mixing processes at the beginning of the simulation cannot be explained physically. The limitation regarding the onset might be caused by the empirical basis of the exchange coefficients, which might result in deviations of the simulation when modeling dense situations. For a steady-state process, the limitation is neglectable.

To avoid the maximum packing limit in combination with the total segregation of both granular phases, a continuous simulation setup was used, in which only the pure material was layered in the feed frame. The tracer was fed constantly across the entire inlet in the geometry. The profiles of the tracer weight fraction w_{tracer} at the outlet and F for three rotational speeds are presented in Fig. 4 (DI-CAFOS) and Fig. 5 (MCC).

For the simulations as well as the experiments, the tracer fraction increased with increasing time until a maximum tracer fraction was reached, since the pure material at the outlet was exchanged by the tracer material. This mixing process was pro-

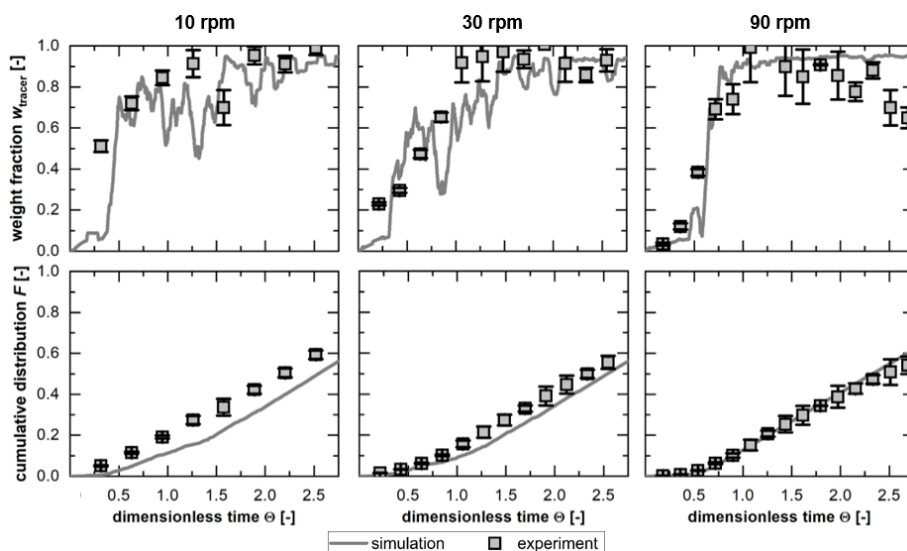


Figure 4. Simulated (sliding average: 2 s) and experimentally determined ($mean \pm s$, $n = 3$) weight fraction of tracer w_{tracer} and cumulative distribution F as function of dimensionless time Θ for a continuous simulation setup and three rotational speeds (material: DI-CAFOS).

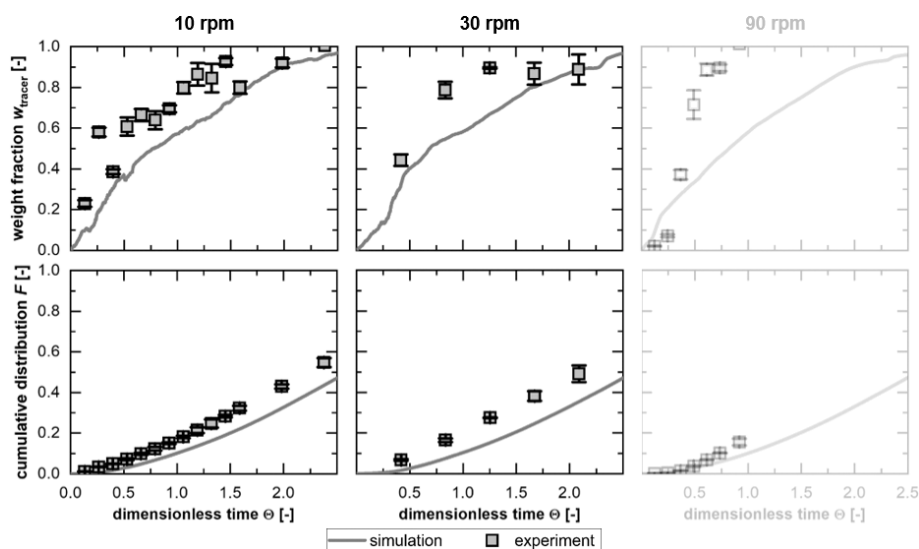


Figure 5. Simulated (sliding average: 2 s) and experimentally determined ($mean \pm s$, $n = 3$) weight fraction of tracer w_{tracer} and cumulative distribution F as function of dimensionless time Θ for a continuous simulation setup and three rotational speeds (material: MCC).

nounced for the free-flowing material (DI-CAFOS) and higher rotational speeds. Unity was not reached by F because of the short measurement period. Furthermore, a strong tailing was observable in the simulated profiles after four hydrodynamic residence times, which indicates the rather high mixing capacity of the feed frame.

Overall, the results of the continuous simulation are in good agreement with the experimentally determined results. Again, the consistency is an indicator for the applicability of the Eulerian approach to describe the mixing behavior of two granular phases. For DI-CAFOS, the increasing and decreasing trends in w_{tracer} were caused by the movement of particle clusters, which was especially relevant for small rotational speeds. The visibility of the trend was less distinct in the results of the experiments due to the low frequency of the measurement and the long sampling time. The overestimation of F for low rotational speeds was a result of the overassessment of the first experimental value. Because of the fast replacement of the powder in combination with the comparably long sampling time, the onset of the experimentally determined profile of F cannot be represented well, which was a limitation solely related to the experiments. For MCC, the increasing and decreasing trends in w_{tracer} were clearly smaller due to the lower flowability. The deviations between simulations and experiments were more distinct for MCC. Here, the phase properties were even more unequal to a continuum compared to DI-CAFOS, based on the lower flowability. Nevertheless, the results of the simulations represent the general trends of w_{tracer} as well as F , except the simulation with the highest rotational speed (90 rpm). In this experiment, an unexpected low mass flow was observed, which indicated a clogging of the outlet. The inadequate representation of this static behavior is in accordance with previous simulations.

3.4 Application of the Eulerian Simulation

Powder RTD in a rotary tablet press feed frame has an impact on the quality of the product. Normally, experiments are necessary to gain knowledge of the RTD as well as a deeper process understanding. Numerical simulations are an alternative to measurements to be more cost- and time-effective. As an example, the mean dimensionless time Θ_{50} and the distribution width, which is described by the interquartile range IQR , of the simulated RTDs in the feed frame are plotted in Fig. 6. The IQR is defined as the ratio of the difference between Θ_{75} and Θ_{25} to Θ_{50} .

As illustrated in Fig. 6, Θ_{50} as well as IQR were nearly constant with respect to the rotational speed of the stir-type agitator and, for both parameters, the differences were insignificant based on a regression analysis ($\alpha = 0.05$). Hence, the rotational speed did not influence the mixing process. This finding is in good agreement with previous studies, in which the influence of the feed frame paddle speed was analyzed experimentally [35]. In conclusion, the Eulerian approach is suitable to describe the powder flow and the mixing process of two granular phases under given constraints.

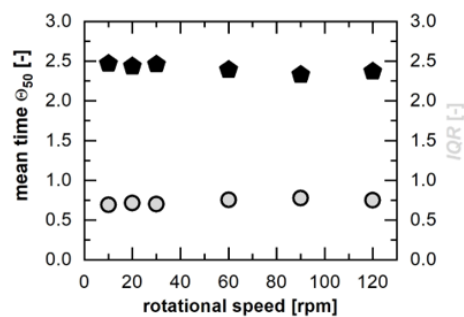


Figure 6. Mean dimensionless time Θ_{50} (black hexagon) and IQR (grey circle) of the simulated RTDs as a function of the rotational speed (material: DI-CAFOS).

4 Conclusion

Within this study, the feasibility of the Eulerian approach, which is an alternative numerical method for describing the powder flow, was demonstrated. In two- and three-dimensional simulations, the behavior of a granular phase was verified by comparison with an experimentally determined powder flow. Using the Eulerian model, no limitations regarding particle size or number were detected. However, the simulation was limited to dynamic conditions, as the effect of clogging cannot be modeled well due to the chosen simulation models.

The feasibility of determining the RTDs in a feed frame by the application of the Eulerian approach was revealed considering particular constraints. The combination of the maximum packing limit and the total segregation of both particulate phases might result in a non-physical overestimation of the mixing process at the beginning of the simulation. Nevertheless, the prediction of the mixing behavior of two granular phases was possible, as the ascending slope of the simulated F profile was in good agreement with the experimental values.

Finally, the applicability of the Eulerian approach in a pharmaceutical context was demonstrated. For increasing cost- and time-effectiveness, the numerical simulation can be used to gain a deeper process understanding, which is demonstrated for the influence of the stir-typed agitator on Θ_{50} and IQR . In accordance with previous experimental studies, neither of the parameters was affected by the rotational speed.

Acknowledgment

The authors are grateful for the assistance of Elizabeth Ely (EIES, Lafayette, USA) in preparing the manuscript. Open access funding enabled and organized by Projekt DEAL.

The authors have declared no conflict of interest.

Symbols used

d_p	[μm]	particle diameter
e	[-]	coefficient of restitution
F	[-]	cumulative density function
IQR	[-]	interquartile range
m	[g]	mass
\dot{m}	[g s^{-1}]	powder mass flow
mean	[various]	arithmetic mean
n	[-]	sample size
r_o	[mm]	radius of the funnel outlet
s	[various]	standard deviation
$t_{\text{discharge}}$	[s]	time of powder discharge
w_{tracer}	[-]	tracer weight fraction

Greek letters

α	[-]	level of significance
β	[$^\circ$]	upper angle of the funnel
γ	[$^\circ$]	angle of internal friction
Θ	[-]	dimensionless time
Θ_i	[-]	dimensionless time to a quantile value of $i\%$
ρ	[kg m^{-3}]	density

Abbreviations

API	active pharmaceutical ingredient
DEM	discrete element method
DI-CAFOS	dicalcium phosphate anhydrate
MCC	microcrystalline cellulose
QbD	quality-by-design
RTD	residence time distribution

References

- [1] *Pharmazeutische Technologie* (Eds: K. H. Bauer, K.-H. Frömming, C. Führer), 9th ed., Wissenschaftliche Verlagsgesellschaft, Stuttgart **2012**.
- [2] *Die Tablette: Handbuch der Entwicklung, Herstellung und Qualitätssicherung* (Eds: A. Bauer-Brandl, W. A. Ritschel), 3rd ed., ECV Editio Cantor Verlag, Aulendorf, Germany **2012**.
- [3] R. Mendez, F. Muzzio, C. Velazquez, *Powder Technol.* **2010**, *200*, 105–116. DOI: <https://doi.org/10.1016/j.powtec.2010.02.010>
- [4] R. Mendez, C. Velazquez, F. J. Muzzio, *Powder Technol.* **2012**, *229*, 253–260. DOI: <https://doi.org/10.1016/j.powtec.2012.06.045>
- [5] D. Mateo-Ortiz, R. Méndez, *Powder Technol.* **2015**, *278*, 111–117. DOI: <https://doi.org/10.1016/j.powtec.2015.03.015>
- [6] O. Levenspiel, *Chemical Reaction Engineering*, 3rd ed., John Wiley & Sons, Hoboken, NJ **1999**.
- [7] *ICH Guideline Q8 (R2) on Pharmaceutical Development*, European Medicines Agency, London **2017**.
- [8] L. X. Yu, *Pharm. Res.* **2008**, *25* (4), 781–791. DOI: <https://doi.org/10.1007/s11095-007-9511-1>
- [9] L. Zhang, S. Mao, *Asian J. Pharm. Sci.* **2017**, *12* (1), 1–8. DOI: <https://doi.org/10.1016/j.ajps.2016.07.006>
- [10] J. Rantanen, J. Khinast, *J. Pharm. Sci.* **2015**, *104* (11), 3612–3638. DOI: <https://doi.org/10.1002/jps.24594>
- [11] C.-Y. Wu, *Particuology* **2008**, *6* (6), 412–418. DOI: <https://doi.org/10.1016/j.partic.2008.07.008>
- [12] D. Mateo-Ortiz, F. J. Muzzio, R. Méndez, *Powder Technol.* **2014**, *262*, 215–222. DOI: <https://doi.org/10.1016/j.powtec.2014.04.023>
- [13] W. R. Ketterhagen, *Powder Technol.* **2015**, *275*, 361–374. DOI: <https://doi.org/10.1016/j.powtec.2015.01.073>
- [14] D. Mateo-Ortiz, R. Méndez, *Adv. Powder Technol.* **2016**, *27* (4), 1597–1606. DOI: <https://doi.org/10.1016/j.appt.2016.05.023>
- [15] S. R. Gopireddy, C. Hildebrandt, N. A. Urbanetz, *Powder Technol.* **2016**, *302*, 309–327. DOI: <https://doi.org/10.1016/j.powtec.2016.08.065>
- [16] C. Hildebrandt, S. R. Gopireddy, R. Scherließ, N. A. Urbanetz, *Adv. Powder Technol.* **2018**, *29* (3), 765–780. DOI: <https://doi.org/10.1016/j.appt.2017.12.019>
- [17] C. Ramirez-Aragón, F. Alba-Elías, A. González-Marcos, J. Ordieres-Meré, *Powder Technol.* **2018**, *328*, 452–469. DOI: <https://doi.org/10.1016/j.powtec.2018.01.054>
- [18] E. Siegmann, T. Forgber, P. Toson, M. C. Martinetz, H. Kureck, T. Brinz, S. Manz, T. Grass, J. Khinast, *Adv. Powder Technol.* **2020**, *31* (2), 770–781. DOI: <https://doi.org/10.1016/j.appt.2019.11.031>
- [19] P. A. Cundall, O. D. L. Strack, *Géotechnique* **1979**, *29* (1), 47–65. DOI: <https://doi.org/10.1680/geot.1979.29.1.47>
- [20] Z. Y. Zhou, S. B. Kuang, K. W. Chu, A. B. Yu, *J. Fluid Mech.* **2010**, *661*, 482–510. DOI: <https://doi.org/10.1017/S002211201000306X>
- [21] C. A. Radeke, B. J. Glasser, J. G. Khinast, *Chem. Eng. Sci.* **2010**, *65* (24), 6435–6442. DOI: <https://doi.org/10.1016/j.ces.2010.09.035>

- [22] C. Hildebrandt, S. R. Gopireddy, R. Scherließ, N. A. Urbanetz, *Powder Technol.* **2019**, *345*, 616–632. DOI: <https://doi.org/10.1016/j.powtec.2019.01.040>
- [23] C. H. Ibsen, E. Helland, B. H. Hjertager, T. Solberg, L. Tadríst, R. Occelli, *Powder Technol.* **2004**, *149* (1), 29–41. DOI: <https://doi.org/10.1016/j.powtec.2004.09.042>
- [24] P. Patro, S. K. Dash, *Powder Technol.* **2014**, *264*, 320–331. DOI: <https://doi.org/10.1016/j.powtec.2014.05.048>
- [25] D. A. Santos, C. R. Duarte, M. A. S. Barrozo, *Powder Technol.* **2016**, *294*, 1–10. DOI: <https://doi.org/10.1016/j.powtec.2016.02.015>
- [26] M. Chen, M. Liu, Y. Tang, *Int. J. Chem. React. Eng.* **2019**, *17* (7), 20180254. DOI: <https://doi.org/10.1515/ijcre-2018-0254>
- [27] ANSYS CFX *Fluent Theory Guide*, Ansys, Inc., Canonsburg, PA **2021**.
- [28] O. Gryczka, S. Heinrich, N. G. Deen, M. van Sint Annaland, J. A. M. Kuipers, M. Jacob, L. Mörl, *Chem. Eng. Sci.* **2009**, *64*, 3352–3375. DOI: <https://doi.org/10.1016/j.ces.2009.04.020>
- [29] L. Schiller, Z. Naumann, *Z. Ver. Dtsch. Ing.* **1935**, *77*, 318–320.
- [30] C. K. K. Lun, S. B. Savage, D. J. Jeffrey, N. Chepuruiy, *J. Fluid Mech.* **1984**, *140*, 223–256. DOI: <https://doi.org/10.1017/S0022112084000586>
- [31] D. Gidaspow, *Multiphase Flow and Fluidization*, 1st ed., Academic Press, San Diego, CA **1994**.
- [32] D. G. Schaeffer, *J. Differ. Equations* **1987**, *66* (1), 19–50. DOI: [https://doi.org/10.1016/0022-0396\(87\)90038-6](https://doi.org/10.1016/0022-0396(87)90038-6)
- [33] R. Bharadwaj, C. Smith, B. C. Hancock, *Int. J. Pharm.* **2010**, *402* (1–2), 50–56. DOI: <https://doi.org/10.1016/j.ijpharm.2010.09.018>
- [34] P. Grohn, D. Weis, M. Thommes, S. Heinrich, S. Antonyuk, *Chem. Eng. Technol.* **2020**, *43* (5), 887–895. DOI: <https://doi.org/10.1002/ceat.201900517>
- [35] M. Zimmermann, M. Thommes, *Drug Dev. Ind. Pharm.* **2021**, *47* (5), 790–798. DOI: <https://doi.org/10.1080/03639045.2021.1934871>